

# Dynamic Fracture of Silicon: Concurrent Simulation of Quantum Electrons, Classical Atoms, and the Continuum Solid

Farid F. Abraham, Noam Bernstein,  
Jeremy Q. Broughton, and Daryl Hess

## Introduction

Our understanding of materials phenomena is based on a hierarchy of physical descriptions spanning the space-time regimes of electrons, atoms, and matter and given by the theories of quantum mechanics, statistical mechanics, and continuum mechanics. The pioneering work of Clementi and co-workers<sup>1</sup> provides a lucid example of the traditional approach to incorporating multiscale phenomena associated with these three mechanics. Using quantum mechanics, they evaluated the interactions of several water molecules. From this data base, they created an empirical potential for use in atomistic mechanics and evaluated the viscosity of water. From this computed viscosity, they performed a fluid-dynamics simulation to predict the tidal circulation in Buzzard's Bay. This is a powerful example of the sequential coupling of length and time scales: a series of calculations is used as input to the next rung up the length/time-scale ladder.

However, there are situations where the physics on different length scales interacts dynamically, and an adequate description is not possible using the sequential-coupling scheme employed by Clementi.

Dynamic fracture is a very good example. Energy from large-scale elastic fields is concentrated on the angstrom scale of the electrons that participate in atomic bonding. A simulation of this phenomenon requires an accurate description of atoms bonding at the crack tip, while at the same time including a proper description for very large volumes of strained material, the resolution varying with distance from the crack tip. Far away, it is adequate to use the equations of motion for a macroscopic-averaged continuum field. With decreasing distance from the crack tip, singularities in the elastic field are cut off by atomic-scale phenomena and the eventual breaking of electronic bonds. These phenomena on the one hand require more information to describe, but on the other hand, they dominate in successively smaller regions of materials. This suggests a natural physical-domain decomposition:  $\text{\AA}^3$  volumes where electronic excitations must be considered explicitly,  $\text{nm}^3$  regions where atomic processes must be described, and  $>\mu\text{m}^3$  regions where displacement fields are sufficient. This spatial decomposition makes it possible to combine different

simulation methods describing the different physical regions into a single, powerful simulation tool.

We present a method that *dynamically* couples continuum mechanics far from the crack, empirical potential MD near the crack, and quantum tight-binding (TB) dynamics at the crack tip, to simulate fracture in silicon. Continuum mechanics has long been fruitfully applied to the study of fracture<sup>2</sup> by explicitly putting in pre-existing cracks or a phenomenological description of material decohesion. We use it to efficiently describe large parts of the system that are elastically deformed but do not include highly strained or broken bonds. Closer to the crack, as the strains become larger and the continuum description becomes less accurate, empirical potential molecular dynamics (MD) provides a fast atomistic description. While MD can be used to simulate fracture by itself,<sup>3,4</sup> the empirical potentials that govern the interaction between atoms may not reliably describe the breaking of bonds at the crack tip. A more accurate description in this region is given by TB dynamics, a method that simulates classical nuclei interacting via a simple quantum-mechanical description of the electrons that form interatomic bonds.

In the next section, we will describe the multiscale simulation method called MAAD,<sup>5</sup> discuss new refinements of the method, and present new results for the dynamic fracture of silicon that differ significantly from our original simulation results. Employing a new TB technique, we observe interplanar brittle cleavage with no surface roughening. This is in contrast to our earlier simulation,<sup>5</sup> where we observed surface roughening at the two tips of an interior crack, one tip being described by an inaccurate multicluster TB approximation and the second tip by the empirical silicon potential of Stillinger-Weber. This new simulation agrees with experiment.

We give a very brief listing of other relevant studies addressing multiscale simulation methods. Kohlhoff and co-workers<sup>6</sup> have coupled continuum mechanics and atomistic dynamics in an early fracture-simulation investigation. An independent implementation for coupling the continuum and atomistic regimes was given by Hoover.<sup>7</sup> Another recent study describing a method for interfacing these two regimes is by Ruffi-Tabar et al.<sup>8</sup> A non-dynamical formalism bringing atomic information into the continuum mechanics of deformation is described by Shenoy and co-workers.<sup>9</sup> In a paper by Capaz et al.,<sup>10</sup> a MD/TB coupling scheme is employed to predict equilibrium structure.

A review of the issues involved in coupling quantum systems to classical force fields is given by Vanduijn and Devries.<sup>11</sup> We are unaware of any study coupling all three regimes either concurrently or dynamically.

## The Original MAAD Method

We have invented a method for *dynamically coupling the length scales*<sup>5</sup> and applied it to the rapid brittle fracture of a silicon slab under uniaxial tension. A seed crack is placed at its center. The slab is partitioned into five regions of the simulation (Figure 1). The natural physical-domain decomposition of fracture suggests a computational-domain decomposition for parallel computers. Far from the crack, we use continuum linear elasticity treated by the finite-element (FE) method.<sup>12</sup> One processor is used for each of the two FE regions. Around the crack, with large strains but with no bond rupture, we use empirical potential MD, which integrates Newton's equations of motion given the interatomic forces. The force law between silicon atoms is derived from the Stillinger–Weber potential.<sup>13</sup> We have also used the environment-dependent interatomic potential (EDIP) of Kaxiras and co-workers<sup>14</sup> with similar results. Because MD has a large computational burden, we further partition this region spatially and distribute the computational load onto several processors. Lastly, in the region of bond failure at the crack tip, we use the TB method to provide a quantum-mechanical description of the electrons that participate in bonding. Forces derived from TB drive the dynamics of the nuclei, which are described by classical degrees of freedom. For this silicon study, we use the nonorthogonal TB parameterization of Bernstein and Kaxiras.<sup>15</sup> In the approach discussed in Reference 5, a cluster of eight small TB subregions was used to speed up the calculations for the TB region, which is the most computationally demanding part of the overall code. We track the path of the crack and place the center of the TB region at the apex of the crack, where the bond-breaking occurs. We have since found that this overlapping TB cluster scheme is inaccurate and makes the TB region behave more like a region of Stillinger–Weber atoms. As a result, the TB crack tip and the Stillinger–Weber crack tip had essentially identical dynamics. We now use a single TB cluster of atoms. This guarantees that the TB region is composed of TB atoms with no contamination from empirical atoms.

Two crucial aspects of our original procedure are the handshaking algorithms between the FE and the MD method and

between the MD and the TB methods, where *seamless* couplings are required.<sup>5</sup> In FE regions far from the FE/MD boundary, we use a coarse mesh describing a large continuum solid. In the FE/MD handshake region (Figure 2), the FE mesh spacing is scaled to atomic dimensions. The handshaking is accomplished by taking the interaction energy across the FE/MD boundary as the mean of the FE linear elastic description and the MD interatomic potential description. The time-dependent displacement field at each mesh point in the FE region is computed from the time-integration of the generalized equations of motion of continuum elastic theory. A time-integration algorithm identical to that used in conventional MD is used so that the nodes in the FE description of the displacement field are dynamical variables that follow in lockstep with those of their atomic cousins in the MD region. The FE/MD interface is chosen to be far from the fracture region, so that MD atoms and the nodes of the FE mesh can be unambiguously assigned to one another.

For the MD/TB handshake interface (Figure 3), dangling bonds at the edge of the TB region are passivated with special terminating atoms. These are fictitious atoms that interact with the electrons of the silicon atoms at the surface of the region so as to tie off a single bond each, minimizing the effects of the surface on the forces inside the cluster. The TB terminating atoms bond like silicon, but are monovalent like hydrogen, hence the name “silogens.” At the surface of the TB region, we place silogens that sit directly on top of the atoms of the MD simulation. The Stillinger–Weber force is computed for these boundary atoms considering only bonds to atoms in the MD region. The contribution from the missing bonds is accounted for by adding the force computed for each silogen to the atom it represents. As before, the atomic positions of the TB atoms are updated in lockstep with their FE and MD cousins. The entire procedure is formulated in such a way that the simulation, in the absence of dynamic TB tracking of the crack front, conserves total energy.

## Improved Embedding of the TB Region

The original method for treating the TB region in the coupling of length-scale formalism<sup>5</sup> traded accuracy for simulation speed and enabled a first look at dynamics driven at the electronic scale. Enhanced speed is obtained from the way the large TB region is split up into separate subregions; this has the side effect of diluting

the TB forces by averaging them with Stillinger–Weber forces. We have developed a new method<sup>16</sup> for computing the forces in the TB region that does not suffer from this deficiency, but is presently computationally more expensive in practice. Computational effort for this method scales linearly with the number of atoms, and therefore, the TB region does not need to be split into smaller subregions. We emphasize that the TB model of Bernstein and Kaxiras<sup>15</sup> is still adopted; it is the numerical implementation that is different.

Our previous approach for describing the TB region was formulated in terms of electronic eigenvalues and eigenvectors. These quantities require a dense matrix to store, and the computational effort to compute them scales as the number of atoms cubed. The new TB solver can be viewed in terms of the density matrix of the occupied electronic states. This matrix is localized in real space, and can therefore be well approximated by a sparse matrix with a number of nonzero matrix elements proportional to the number of atoms. The density matrix itself is computed by summing a Green's function matrix formed from Hamiltonian and overlap matrices **H** and **S**:

$$\mathbf{G}(z) = (\mathbf{H} - z\mathbf{S})^{-1}, \quad (1)$$

evaluated at a small number of complex energies  $z_i$ . These values are the poles of an approximation to the Fermi distribution proposed by Nicholson and Zhang.<sup>17</sup> The most computationally demanding part of the calculation is a sparse matrix inversion, which we compute using a biconjugate-gradient algorithm<sup>18</sup> in a time that scales linearly with the number of atoms. While the TB solver described in the previous section depends on monovalent, silicon-like atoms to reduce the effects of the TB region surface on the forces computed within it, the new solver can treat the boundary more naturally. The matrix **G**( $z$ ) is localized in real space, and the TB region boundary (by construction) does not have any broken bonds. We can therefore approximate the values of the **G**( $z$ ) matrix elements in the boundary region by values from an ideal system. We then perform an approximate matrix inversion, while constraining the matrix elements involving atoms at the TB region boundary. The full details of this method will be published elsewhere.<sup>16</sup>

Using this solver for a TB/MD region dynamically coupled to a surrounding MD region is straightforward. A layer approximately two atoms thick surrounds the region that is to be described with TB and forms the boundary where matrix ele-

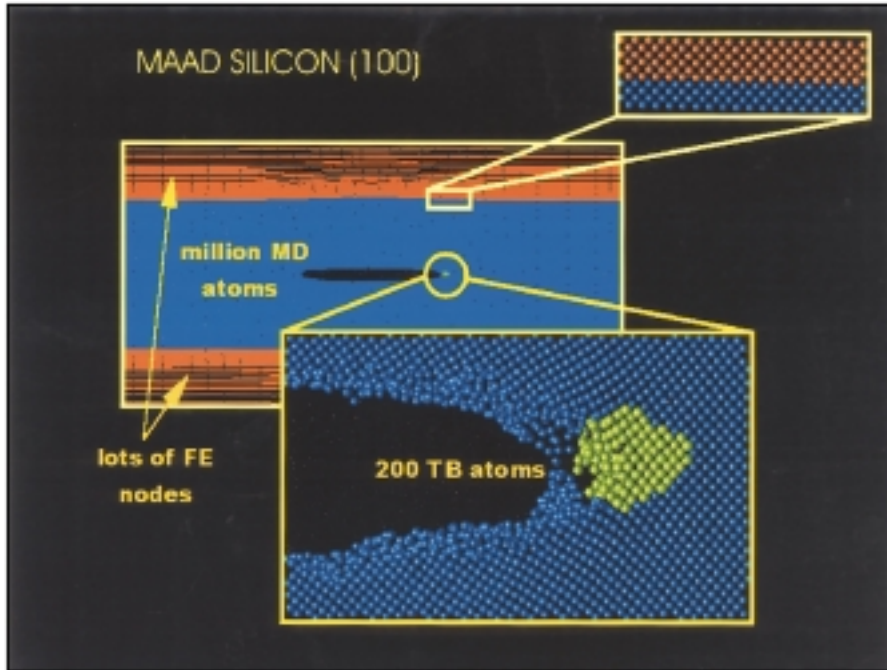


Figure 1. The geometrical decomposition of a silicon slab into the five different dynamic regions of the simulation: the continuum finite-element (FE) region, which is not shown in its entire extent; the atomistic molecular-dynamics (MD) region; the quantum tight-binding (TB) region; the FE/MD “handshaking” interface; and the MD/TB “handshaking” interface. The image is the simulated silicon slab, with expanded view of the TB region surrounded by MD atoms. Note that the TB region surrounds the crack tip with broken-bond MD atoms trailing behind this region.

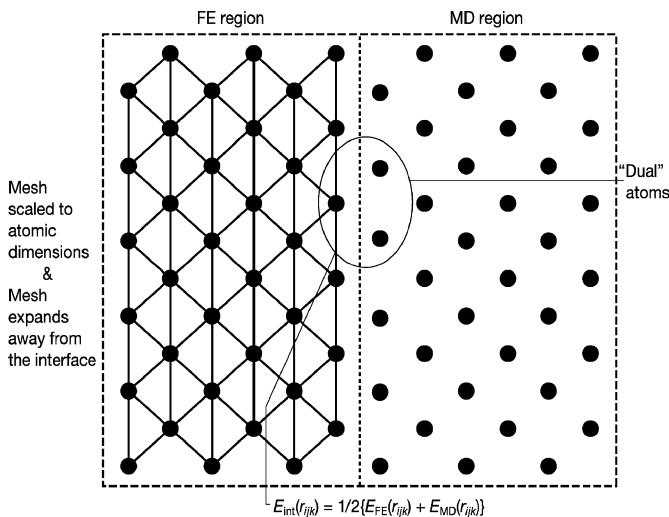


Figure 2. Illustration of FE/MD handshake Hamiltonian. The energy of the three dual atoms  $E_{int}$  at their relative position  $r_{jk}$  equals the mean of the energies, assuming that they are finite-element nodes  $E_{FE}$  or are empirical molecular-dynamics atoms  $E_{MD}$ .

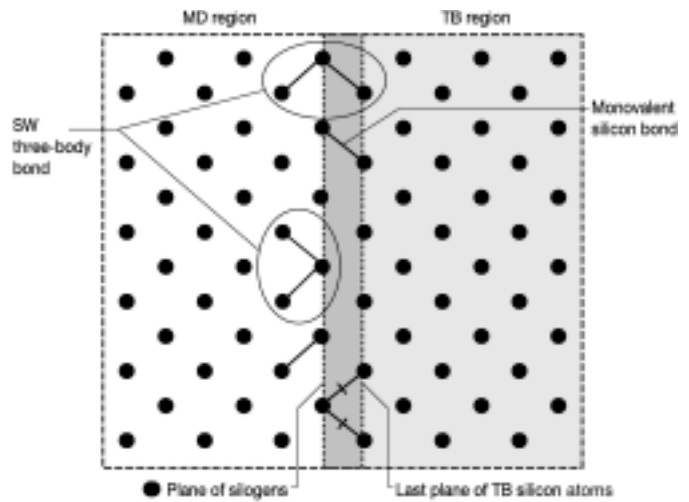


Figure 3. Illustration of original MD/TB handshake Hamiltonian. The TB Hamiltonian is diagonalized for the sum of light-gray + dark-gray regions. Si-Si interactions are employed in the light-gray area, and Si-silogen interactions are used in the dark-gray region. Two- and three-body Stillinger-Weber interactions contributing to handshake Hamiltonian are denoted by solid lines. Broken lines represent noncontributing Stillinger-Weber three-body terms. Only representative Stillinger-Weber examples are shown.

ments are constrained. Since the TB forces in the boundary region are unphysical, they are ignored, and the boundary atoms follow trajectories driven by empirical interatomic forces. No averaging of forces derived from TB and empirical potentials occurs within the TB region itself. In analogy with images of the strain waves propagating through the MD/FE boundary in Figure 6, we tested this embedding method by sending a compression wave through a spherical TB region in a large empirical potential MD system. In Figure 4, we show the elastic energy field as the wave front is going through the center of the TB region. The image shows good continuity, with only minimal effects by the boundary. Because the elastic constants in the two regions are not exactly matched, some refraction of the propagating wave occurs. This effect is quite small, and our test shows that the new embedded TB solver is well coupled to the MD region.

### Application to Fracture

In Figure 5, we present the energy-strain and stress-strain relations for bulk silicon as predicted using the Stillinger-Weber empirical potential and the TB method. Uniaxial tension is applied to the bulk silicon, with the additional constraint that the interatomic separations change by simple scaling in the three cartesian directions. The crystal is stretched in the (100) direction. We note that the Stillinger-

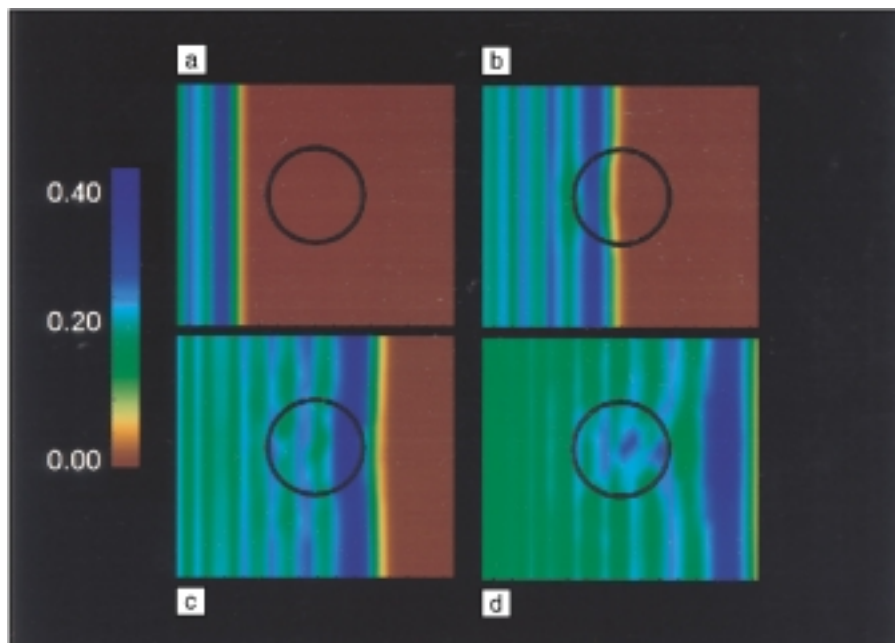


Figure 4. Images from a simulation of a compression wave propagating through a cylindrical TB region embedded in a larger MD region, using the order (N) TB solver, where N is the number of TB atoms. The first image (a) shows the system before the wave has entered the TB region in the middle of the image. (b) and (c) show the system when the wave is in the TB region, and (d) shows it after passing to the other side. Colors represent elastic energy, proportional to the square of the atomic displacement from the ideal positions.

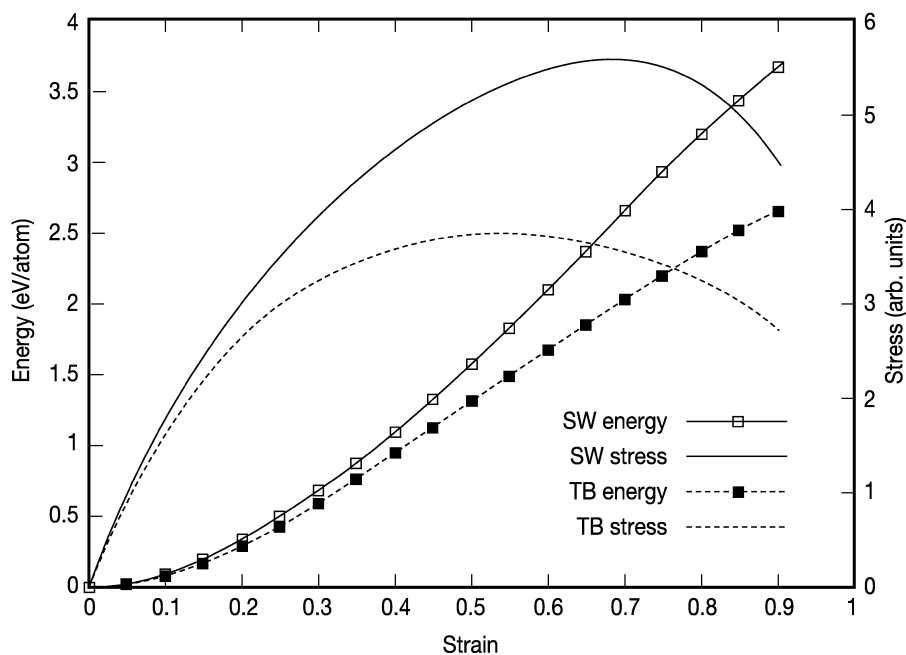


Figure 5. Energy-strain and stress-strain relations for bulk silicon as predicted using the Stillinger–Weber empirical potential and the TB method.

Weber behavior and the TB behavior differ significantly in the hyperelastic regime that governs materials failure at a crack tip. Since the mechanical stability limit

occurs at a lower strain using TB, it is reasonable to expect that a crack tip of TB atoms will fail for a smaller strain than a crack tip of Stillinger–Weber atoms. Also,

this comparison suggests that the empirical potentials should be fitted to the hyperelastic features of a bulk solid when the interest is to simulate materials failure by empirical potential MD. An important step would be to obtain a reliable database from accurate quantum-mechanical calculations (density-functional theory) in the hyperelastic region, so that such a program may be carried out. Of course, this would also provide an effective tool for evaluating empirical potentials and TB schemes. For now, we are assuming that our adopted TB scheme is accurate in the hyperelastic regime.

Using our method for *dynamic coupling of length scales*, we have simulated the fracture of silicon. We create a thin crack in single-crystal silicon samples with either (111) or (100) faces. The system is periodic in the direction perpendicular to the loading direction and crack length. For example, for the system with (100) faces, the thickness is of the order of 11 Å. The MD region is about 800 Å long in the loading direction and about 3500 Å long parallel to the length of the crack. The full system, including the MD and FE regions, is about 4000 Å long in the loading direction. The FE region describes a system four times larger than the MD region, while increasing the number of degrees of freedom by only 20% and *without significantly increasing the computational effort*. When active, the TB region is moved to remain centered around the crack tip every 10 time steps. The simulation is started by imposing a constant strain rate across the pre-cracked sample.

In Figure 6, we show stress waves propagating through the slab by variations in color that correspond to potential energy variations. The stress waves passing from the MD regions to the FE regions show no visible reflection at the FE/MD interface; that is, the coupling of the MD region with the FE region appears seamless. For this simulation, a cluster of eight small TB subregions was used to speed up the calculations for the TB region, but this overlapping TB cluster scheme is inaccurate and makes the TB region behave more like a region of Stillinger–Weber atoms. As a result, the TB crack tip and the Stillinger–Weber crack tip had essentially identical dynamics. The propagating crack tips rapidly achieve a limiting speed (2770 m/s) equal to 85% of the Rayleigh speed, the sound speed of the solid silicon surface. We note that the traveling crack surfaces are rough and disordered for both crack tips, consistent with the statement that the “small multicluster” TB approximation results in a behavior very much like a region of Stillinger–Weber atoms. Marder and

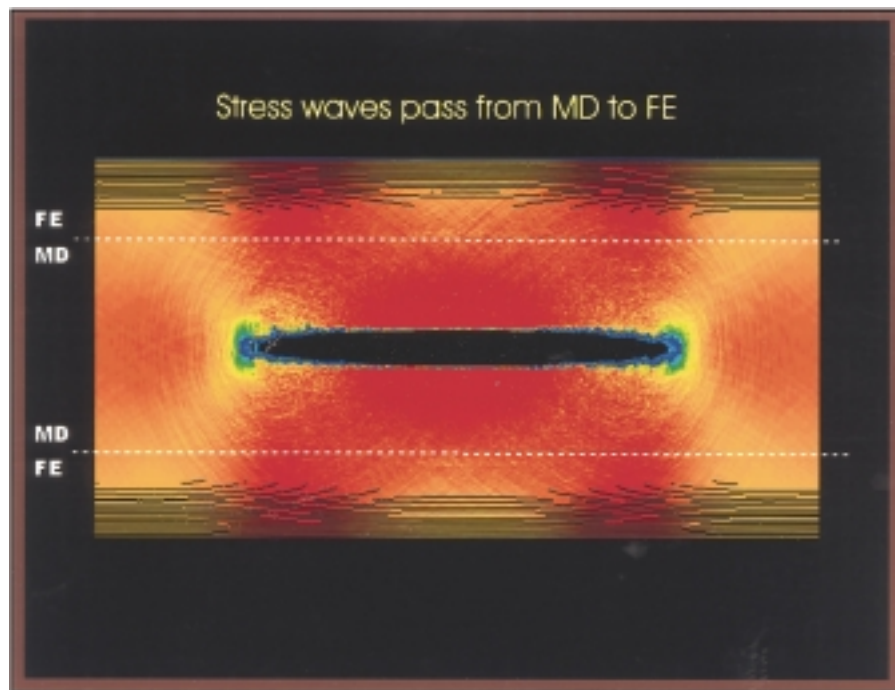


Figure 6. Elastic energy waves propagating through the slab, visualized using a potential-energy color scale. The waves pass through the MD/FE coupling interface with no visible reflection.

colleagues discovered that the Stillinger-Weber potential did not simulate brittle fracture via cleavage<sup>19</sup> and that increasing the repulsive three-body term by a factor of two would produce cleavage in their simulations.

Using the linear-scaling TB method, we have embedded a single large TB cluster in an MD simulation with the EDIP interatomic potential.<sup>14</sup> In this simulation, we have for the first time simulated the brittle fracture of silicon proceeding via interplanar cleavage (Figure 7). The TB crack tip starts propagating at a bulk strain of 2.5%, while a Stillinger-Weber crack tip requires a bulk strain above 8%, consistent with the stress-strain behaviors in Figure 6. Unlike this MAAD brittle cleavage, empirical-potential MD simulates a blunting crack accompanied by significant atomic disorder. We have only very recently begun these simulations, and a quantitative analysis is under investigation.<sup>20</sup>

## Summary

We have presented a simulation approach for physical problems that span a wide range of length scales using brittle fracture as an example application. This paper clearly demonstrates that the MAAD approach is in a dynamic period of development. Future studies may likely apply more sophisticated computational tech-

niques to simulate the three regions, invent more robust procedures for interfacing the three regions, and address physical problems very different from this present study. The concurrent spanning of the continuum to the quantum should prove to be a powerful approach in computational physics.

## Acknowledgments

The original MAAD scientists were Jeremy Broughton, now at Yale School of Management; Noam Bernstein, Division of Engineering and Applied Sciences, and Tim Kaxiras, Division of Engineering and Applied Sciences and Department of Physics at Harvard University; and Farid Abraham, IBM Almaden Research Center. We thank the U.S. Department of Defense High-Performance Computing and Modernization Program for a Grand Challenge grant of computer time at the USAF Maui High-Performance Computing Center, and the ASC Major Shared Resource Center at Wright-Patterson Air Force Base. We acknowledge additional computational support from the San Diego Supercomputer Center, which receives its major funding from the U.S. National Science Foundation. Noam Bernstein acknowledges the sup-

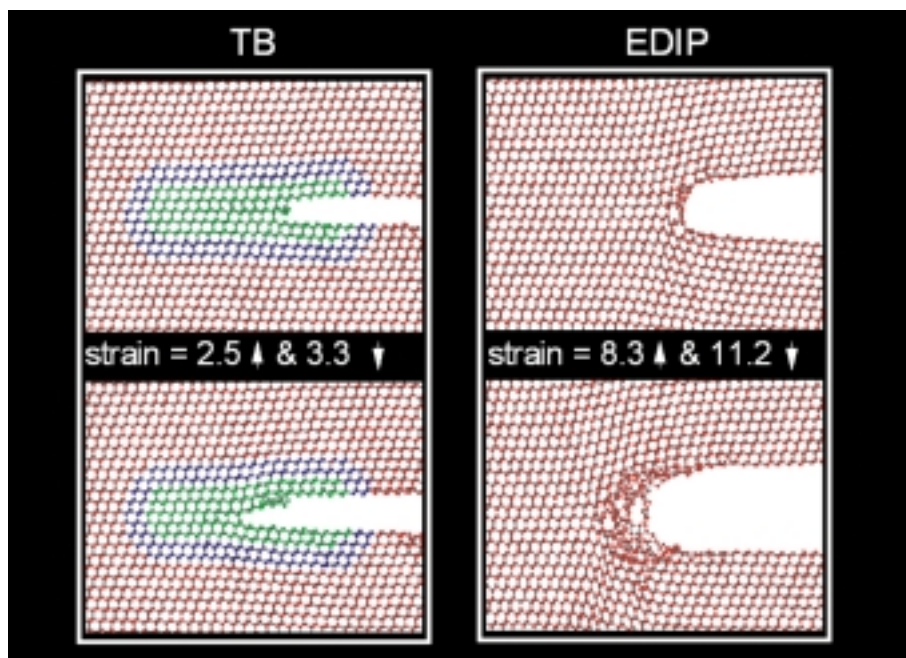


Figure 7. Comparison of crack propagation in silicon using TB atoms (left-hand column) and environment-dependent interatomic potential (EDIP) atoms (right-hand column) for the crack tip, respectively. Using TB, we see brittle fracture proceeding via interplanar cleavage. The top and bottom images in each column are at 2.5% and 3.3% strains, respectively. Red atoms are treated only with the empirical potential, green atoms are treated only with TB, and blue atoms form the boundary between the two regions. Using EDIP, we see crack motion initiating at a much higher strain (8.3%) and proceeding with blunting and significant disorder.

port of the National Research Council Associateship Program. Daryl Hess acknowledges the support of the Office of Naval Research.

### References

1. E. Clementi, *Philos. Trans. R. Soc. London, Ser. A* **326** (1988) p. 445.
2. L.B. Freund, *Dynamic Fracture Mechanics* (Cambridge University Press, New York, 1990).
3. F.F. Abraham, D. Brodbeck, R.A. Rafey, and W.E. Rudge, *Phys. Rev. Lett.* **73** (1994) p. 272; F.F. Abraham, D. Schneider, B. Land, D. Lifka, J. Skovira, J. Gerner, and M. Rosenkrantz, *J. Mech. Phys. Solids* **45** (1997) p. 1461.
4. A. Nakano, R.K. Kalia, and P. Vashishta, *Phys. Rev. Lett.* **75** (1995) p. 3138; A. Omeltchenko, J. Yu, R.K. Kalia, and P. Vashishta, *Phys. Rev. Lett.* **78** (1997) p. 2148.
5. F.F. Abraham, J.Q. Broughton, N. Bernstein, and E. Kaxiras, *Comput. Phys.* **12** (1998) p. 538; *Europhys. Lett.* **44** (1998) p. 783.
6. S. Kohlhoff, P. Gumbsch, and H.F. Fischmeister, *Philos. Mag. A* **64** (4) (1991) p. 851.
7. W. Hoover, A. De Groot, and C. Hoover, *Comput. Phys.* **6** (1992) p. 155.
8. H. Rafii-Tabar, L. Hua, and M. Cross, *J. Phys.: Condens. Matter* **10** (1998) p. 2375.
9. V. Shenoy, R. Miller, E. Tadmor, and R. Phillips, *Phys. Rev. Lett.* **80** (1998) p. 742.
10. R. Capaz, K. Cho, and J. Joannopoulos, *Phys. Rev. Lett.* **75** (1995) p. 1811.
11. P. Vanduijnen and A. Devries, *Int. J. Quantum Chem.* **60** (1996) p. 1111.
12. T. Hughes, *The Finite Element Method* (Prentice-Hall, Englewood Cliffs, NJ, 1987).
13. F.H. Stillinger and T.A. Weber, *Phys. Rev. B* **31** (1985) p. 5262.
14. M.Z. Bazant, E. Kaxiras, and J.F. Justo, *Phys. Rev. B* **56** (1997) p. 8542; J.F. Justo, M.Z. Bazant, E. Kaxiras, V.V. Bulatov, and S. Yip, *Phys. Rev. B* **58** (1998) p. 2539.
15. N. Bernstein and E. Kaxiras, *Phys. Rev. B* **56** (1997) p. 10488.
16. N. Bernstein, in preparation.
17. D.M.C. Nicholson and X.-G. Zhang, *Phys. Rev. B* **56** (1997) p. 12805.
18. W.H. Press, S.A. Teukolsky, W.T. Vetterling, and B.P. Flannery, *Numerical Recipes in C: The Art of Scientific Computing*, 2nd ed. (Cambridge University Press, Cambridge, UK, 1992).
19. J.A. Hauch, D. Holland, M.P. Marder, and H.L. Swinney, *Phys. Rev. Lett.* **82** (1999) p. 3823.
20. N. Bernstein and D.W. Hess, in preparation. □

**Vacuum Pump  
Vibration Isolators**



NEC Vibration Isolators effectively remove vibration from turbo and cryo pumps.

Model VI-1 is elastomer isolated; Model VI-2 is air-isolated. Both are UHV compatible, have short insertion lengths and high conductance with a wide variety of flanges available.

Contact NEC:

WEB SITE: <http://www.pelletron.com>  
E-MAIL: [nec@pelletron.com](mailto:nec@pelletron.com)

**NEC** National Electrostatics Corp.

7540 Graber Road, P.O. Box 620310,  
Middleton, WI 53562-0310 U.S.A.  
Tel. 608/831-7600 • Fax: 256-4103

Circle No. 7 on Inside Back Cover

www.mrs.org/gateway/

## Access the Materials Gateway on the Materials Research Society Web Site

### Buyers Guides

#### Professional Societies

Materials related associations and organizations

#### Academic Departments

University departments and research centers

#### Government Organizations

Including national laboratories

#### Materials Information

Including Web-based databases

#### Publications

Materials related journals and other publications

#### Educational Resources

Resources on the Web for materials related educational resources

#### Companies

Materials industries

#### USENET Newsgroups

Materials research related discussion groups

#### Materials Related Meetings

Upcoming meetings, conferences, workshops and symposia of interest to materials researchers

#### Materials Related News

Materials related news culled from various sources

#### What is Materials Research?

General information about the field of materials including hyperlinks to educational resources on the Web

#### National Nanotechnology Initiative

Information relevant to materials researchers